

Collapsible-Tube Pulsation Generator for Crossflow Microfiltration: Fatigue Testing of Silicone-Rubber Tubes

D. E. HADZISMAJLOVIC* and C. D. BERTRAM

Graduate School of Biomedical Engineering, University of New South Wales, Sydney 2052, Australia

SYNOPSIS

Fatigue tests have been performed for 18 silicone-rubber tubes operating as the active element of a crossflow pulsation generator. It was found that the silicone-rubber tube can be used as the main part of a cheap and reliable oscillator with good reproducibility of the downstream pressure. The operating life of the tubes was between 146 h and 378 h of continuous work for peak-to-peak downstream pressure amplitude 220 kPa to 310 kPa and frequency 5.2 Hz to 8.5 Hz. © 1996 John Wiley & Sons, Inc.

INTRODUCTION

The use of unsteady flow can lead to significant beneficial effects in increasing heat and mass transfer rates.¹ Several studies have demonstrated that membrane flux is improved by pulsatile flow superimposed on the mean crossflow. The attained enhancement varies widely from study to study as the result of different filtration situations. The results which relate to enhancement by virtue of flow pulsation alone must be distinguished from those relating to the use of specialized crossflow channel geometries in combination with flow pulsation. On the other hand, it is very important to know whether the pulsation is superimposed on laminar or turbulent preexisting flow. Colman and Mitchell² have shown that the combined effects of baffles and pulsation increased membrane flux to up to 20 times than in the absence of both when the preexisting flow was laminar. This measure of filtration improvement can mislead when the basal condition yields a particularly low flux.

High flux increases have been achieved with pulsation and geometry due to inefficiency of mixing in laminar crossflow. Vortical mixing correspondingly provided large gains. Abel et al.³ increased the flux in a dialyser by 114% by pulsation. Finnigan and Howell⁴ got about 200% enhancement when ul-

trafiltering whey in a baffled tubular membrane. Specialized geometries to promote vortical mixing and reduce boundary layer thickness were employed in both studies.

Large improvements of the filtration in the absence of devices to create periodically ejected vortices have been also reported. Stairmand et al.⁵ showed that plasma filtration flux in a flat channel could be increased by 260% by pulsation. Milisic and Bersillon⁶ obtained as much as 400% enhancement of bentonite (clay) filtration in a similar geometry. Almost 100 times the pulsationless flux of albumin in flat-sheet ultrafiltration has been measured by Rodgers and Sparks.⁷ For a crossflow ultrafiltration process for solutions of 1% albumin at pH 7.4, the same authors⁸ have shown that transmembrane pressure pulsing improved permeate flux for low wall shear rates. The permeate flux was 100% higher than the limiting flux values for the nonpulsed cases. Pulsing did not improve flux values for turbulent flow cases. Most recently, Rodgers and Sparks⁹ studied variations in albumin initial concentration, solution pH, and ionic strength. The changes in feed concentration caused the most important difference in flux enhancement due to pulsing.

Most experiments involving pulsatile flow without baffles have shown more modest improvement. Jaffrin et al.¹⁰ showed that plasma filtration flux in hollow-fiber filters increased up to 45%. Ben Amar et al.¹¹ have measured 70% flux enhancement using milk and 140% using wine. Kennedy et al.¹² used tubular membrane to process a sucrose solution by

* To whom correspondence should be addressed.

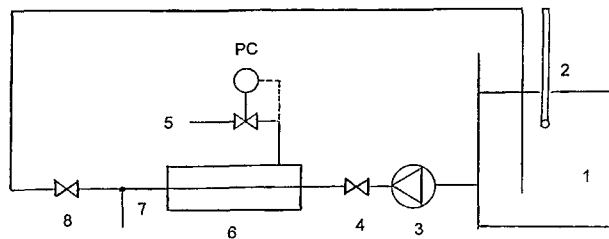


Figure 1 Schematic of the experimental apparatus. 1—Supply vessel with the cooling coil, 2—thermometer, 3—pump, 4—upstream ball valve, 5—compressed air, 6—oscillator, 7—pressure transducer, 8—downstream needle valve.

reverse osmosis and obtained more than 70% enhancement. Their experimental results have been very well followed by the theoretical predictions of Ilias and Govind.¹³ Bauser et al.¹⁴ obtained 38% flux increase for ultrafiltration of whey and 31% for blood. Gupta et al.¹⁵ obtained a flux enhancement of up to 45% using pressure and flow pulsations superimposed on the inlet flow of raw apple juice through a mineral membrane module.

The mechanism in all these studies has apparently been reduction of the extent to which the rejected species in the feedstock accumulates on the

membrane. Depending on the scale of the species, this accumulation is variously known as concentration polarization or as particulate cake. The oscillating flow increases the fluid shear near the membrane surface and may also promote mixing perpendicular to the membrane. These beneficial effects can be achieved on a laboratory scale without pulsatility, by a geometry which promotes vortices,¹⁶ and there are attempts to achieve the same benefits of vortical mixing on an industrial scale.

However, pulsatile flow offers the possibility of delivering these advantages, plus an additional one: the potential to reverse momentarily the transmembrane flux and thereby attack the problem of fouling inside the membrane and its substrate. Wenten et al.¹⁷ have found that good results could be obtained using very short backflush times (typically 0.06 s) with an interval time of 1 to 3 s. The loss of permeate during backflushing was very low. Memtec from Sydney, Australia, uses backflush with the air as the effective method to increase permeate flux. A simple means to interrupt the crossflow periodically and momentarily would provide both the advantages of increased shear and mixing and those of intermittent transmembrane flux reversal. Downstream of the interrupter, the pressure falls as

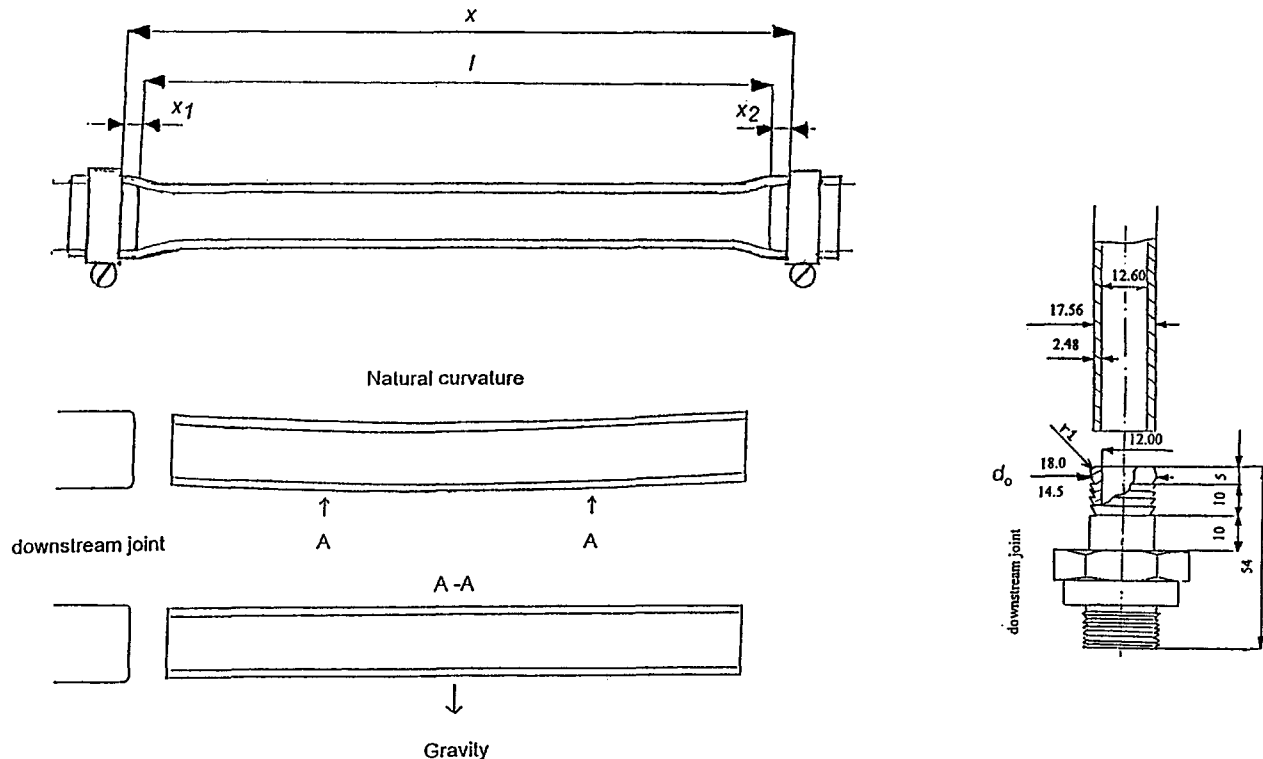


Figure 2 The tube arrangement with details of the downstream joint and the silicone-rubber tube.

Table I Values of Dimensions I , x , x_1 , x_2 , and d_0 (see Fig. 2)

Tube	I (mm)	x (mm)	x_1 (mm)	x_2 (mm)	d_0 (mm)
I	372				18
II	372	380	3.5	4.5	18
III	372	380.5	3.5	5	18
IV	372	383	4.5	6.5	18
V	373	385	5	7	18
VI	376	387.5	6	5.5	18
VII	376	386.5	5.5	5	18
VIII	376	387	5	6	18
IX	376	386	5	5	18
X	382	390	5	3	18
XI	352	367	8	7	18
XII	386	396.5	5.5	5	14.5
XIII	375	386	8	3	14.5
XIV	375.5	385	3.5	6	14.5
XV	369	380.5	6.5	5	14.5
XVI	375.5	383	4	3.5	14.5
XVII	372	380	4.5	3.5	14.5
XVIII	377	385	4	4	14.5

the inertia of the continuing crossflow is arrested, and a reversal of the transmembrane pressure difference can readily be arranged. Since the flux

through the membrane pores is at a low Reynolds number, it follows the instantaneous pressure difference. Such a simple means is presented by a collapsible tube, as used by Bertram et al.¹⁸

Bertram et al.¹⁸ investigated the microfiltration of a dilute suspension of silica particles in water in an unbaffled tubular ceramic membrane. The cross-flow was varied periodically at frequencies inducing fluid-dynamic unsteadiness using a flexible tube compressed to noncircular cross section by external pressure. This arrangement is unstable and leads to self-sustained oscillations, which can be used to add a pulsatile component to a steady flow. With this arrangement and a time-averaged crossflow sufficient for turbulence in the membrane filter, filtrate flux increases due to pulsation of up to 60% were demonstrated, without systematic optimization of the pulse parameters.

Edwards and Wilkinson⁴ and Ilias and Govind¹³ have evaluated the extra power requirement for oscillatory flow and have shown that the gain in transmembrane flux outweighs the cost of extra power. It must be borne in mind that additional capital equipment will be required to produce pulsating flow conditions. Such pulsating flows can be produced by reciprocating pumps or by steady-flow pumps together with some mechanical interrupter device. In

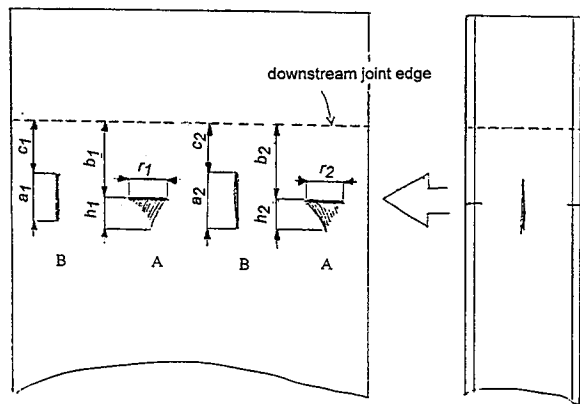
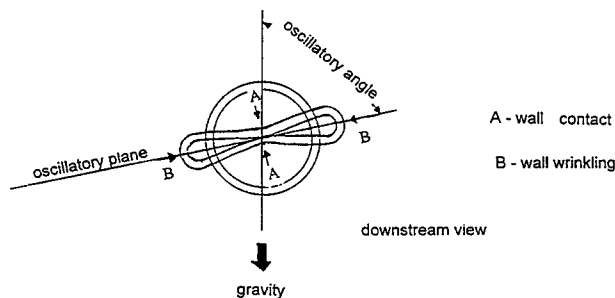


Figure 3 Pulsation scars on the silicone-rubber tubes.

Table II Experimental Values of Young's Modulus E , Mean Air Pressure p_e , Minimum and Maximum Water Temperature T_{min} and T_{max} , and Angle of the Oscillatory Plane α , as defined in Figure 3

Tube	E (MPa)	p_e (kPa)	T_{min} (°C)	T_{max} (°C)	α (deg)
I		200	24.0	52.0	90
II		207	15.0	21.0	45
III		207	15.0	21.0	45
IV		207	15.1	21.4	45
V		207	14.4	22.0	10
VI	3.27	200	15.2	21.3	25
VII	3.46	200	14.8	22.3	90
VIII	3.93	193	14.2	20.3	30
IX	3.92	193	16.7	23.0	20
X	3.95	193	16.5	23.0	25
XI	3.76	169	16.8	23.0	110
XII	4.16	186	16.8	23.8	90
XIII	4.56	179	14.8	22.5	90
XIV	3.51	186	15.6	22.0	45
XV	3.47	179	15.0	23.1	90
XVI	3.83	186	15.7	22.2	135
XVII	3.98	186	15.2	23.2	80
XVIII	3.88	186	14.8	20.1	100

most cases steady-flow pumps are already installed in filtration plants, so an interrupter device would be preferable.

A collapsible-tube pulsation generator is a very simple and cheap oscillator. The self-excited oscillations of collapsed tubes have been extensively analyzed by Bertram¹⁹ and Bertram et al.²⁰⁻²² This device has advantages over previous systems for creating flow pulsation in that there are no sliding parts and only one moving part, and the feedstock does not come in contact with oil or other foreign matter.

The plant complexity of creating an oscillating flow can be reduced to economic proportions through the use of a collapsible-tube self-excited oscillator. The aim of this investigation was to determine the collapsible tube's operating life, reliability, and pulsation reproducibility.

PROCEDURE

The experimental apparatus used for this work is shown schematically in Figure 1. Water recirculated

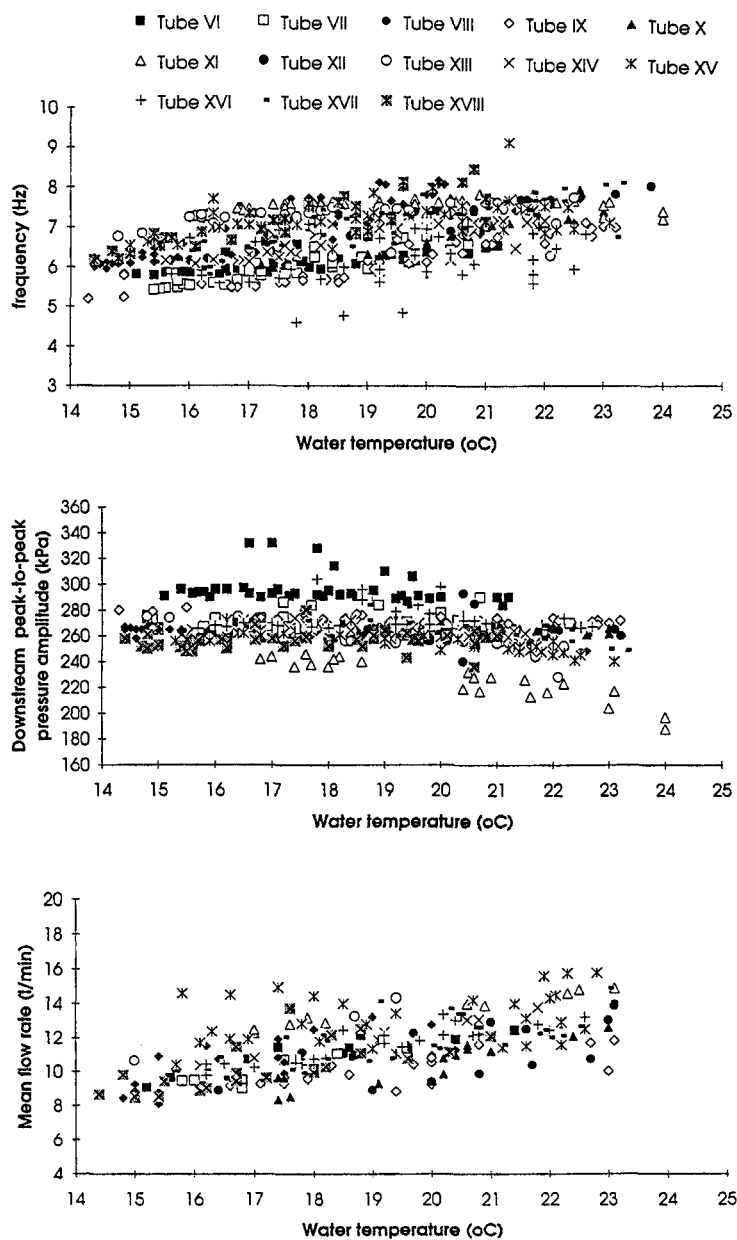


Figure 4 The variation with water temperature of the mean flow rate, oscillation frequency, and peak-to-peak downstream pressure amplitude for tubes with 2% extension.

through a rig consisting of the supply vessel with a cooling coil, a pump (Jebsco 6050-237), the oscillator, an upstream ball valve, and a downstream needle valve, all interconnected by fiber-reinforced flexible hose.

The chamber surrounding the collapsible tube was supplied by compressed air through a pressure regulator. The collapsible-tube oscillator consisted of a horizontally mounted silicone rubber tube. When the air pressure in the surrounding chamber exceeds a critical value, the tube collapses at the downstream end (i.e., the circular cross section becomes an involuted, bi-lobed shape). This results in a smaller cross section for flow and higher pressure drop, causing abrupt retardation of the flow

downstream. The collapse is temporary, because the upstream pressure then forces the tube open again.

The tubes used for the fatigue tests were clear, seamless silicone rubber tubes (Dow Corning Silastic Medical Grade), designed for use in a variety of clinical and laboratory applications. All tubes for the fatigue test were taken from the same tube batch. Nominal internal and outside diameters of the tubes were 12.7 mm and 17.5 mm, respectively. The unstressed tubes had a slightly oval shape. The major and minor measured axis dimensions were 12.87/17.86 mm and 12.33/17.26 mm, respectively. Longitudinal tension versus extension was measured, and Young's modulus was determined for tubes VI to XVIII.

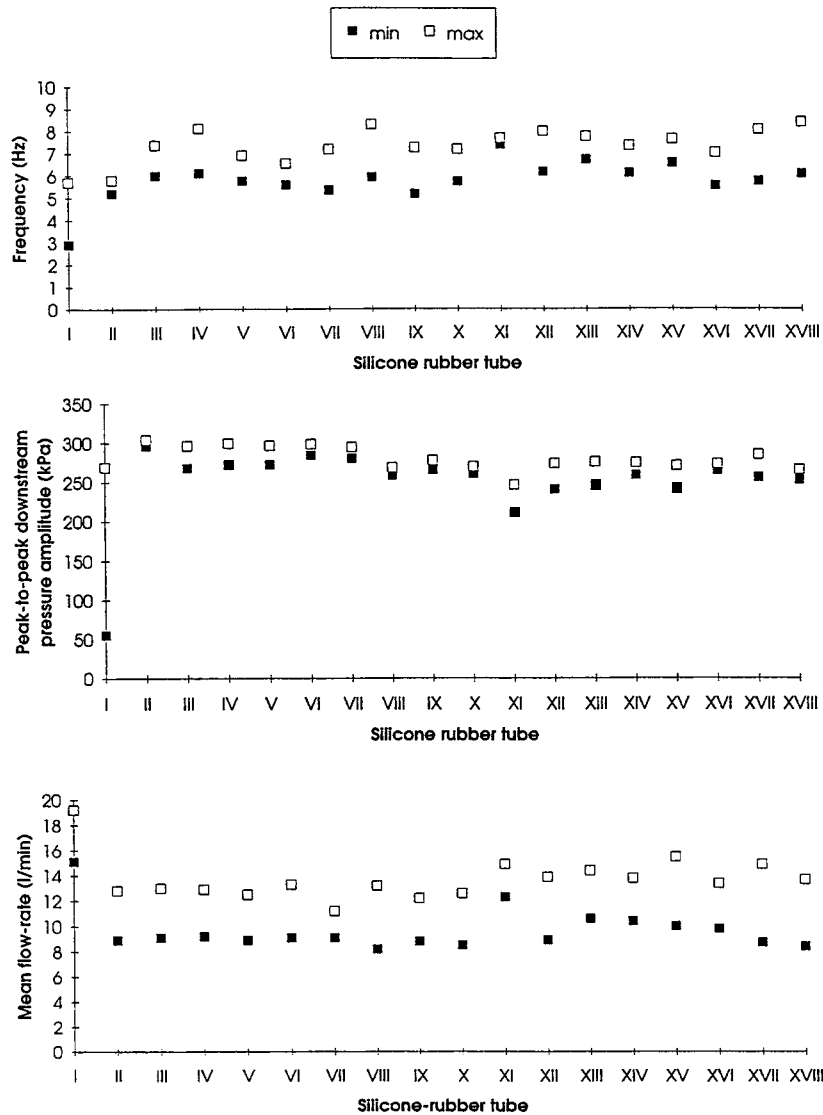


Figure 5 Minimum and maximum values of mean flow rate, pulsation frequency, and peak-to-peak downstream pressure amplitude for all fatigue tests.

The tube was mounted and sealed on the upstream and downstream rigid pipes by steel hose screw clamps of 12 mm width and 0.75 mm thickness. Figure 2 shows the details of this joint. The values of the dimensions l , x , x_1 , x_2 , and d_0 , defined in Figure 2, are given in Table I. The distance between the pipes was between 352 and 386 mm. Tubes I to XI were tested with an 18.0-mm outside-diameter downstream pipe, while the rest had a 14.5-mm downstream pipe. All other dimensions of the joints were identical. The downstream pipe edge was rounded to a radius of 1 mm and polished.

Tubes VI to XVIII were all installed in the same

way with respect to their natural curvature, as shown in Figure 2. Tubes I to V were installed without adjustment of the longitudinal strain, while the rest had 2% longitudinal extension. The pulsations were adjusted by controlling the mean air pressure in the chamber while both valves in the rig were fully open. All fatigue tests were continuous from the beginning to the end of tube operating life. The angle of the oscillatory plane, defined in Figure 3, was measured for each tube. The mean flow rate was determined several times a day by timed water collection.

The downstream pressure was measured by a wideband transducer (Kulite IPT-750-100 SG) in-

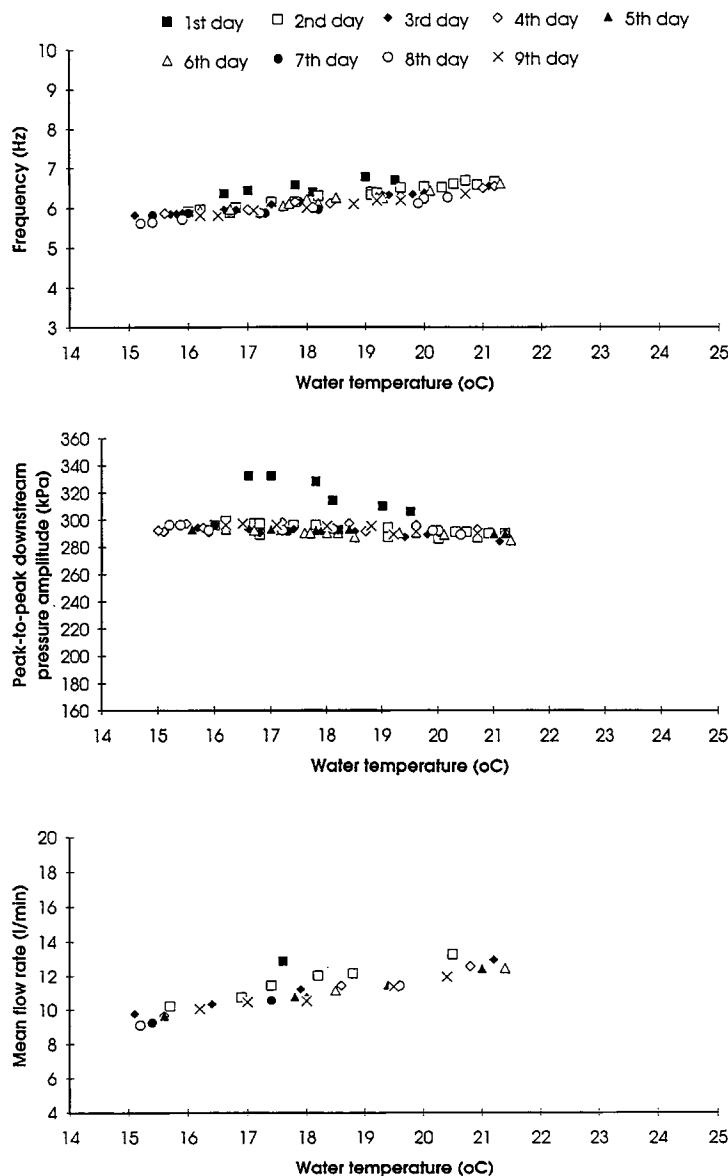


Figure 6 Mean flow rate, frequency, and peak-to-peak downstream pressure amplitude versus water temperature during the fatigue test for tube VI.

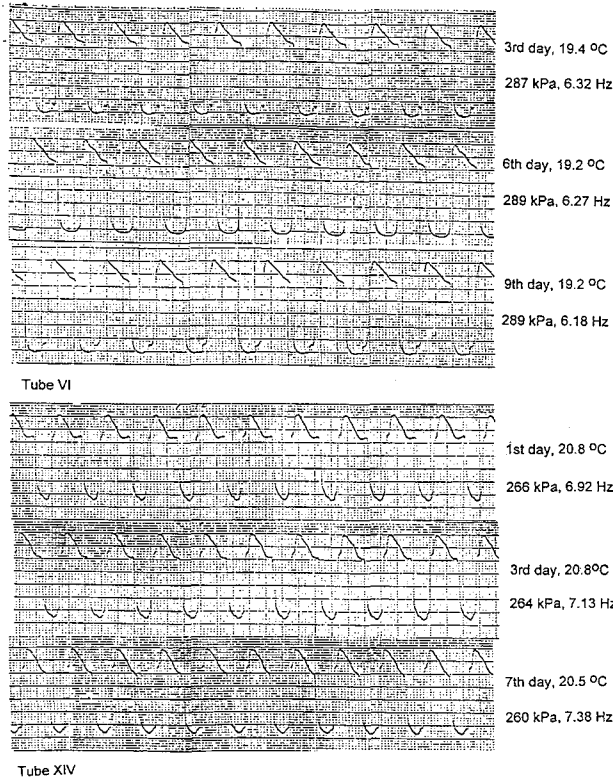


Figure 7 The downstream pressure wave during the fatigue tests for tubes VI and XIV.

stalled 1 m downstream of the exit of the collapsible tube chamber. The instantaneous pressure waveform was recorded several times a day by a fast pen recorder (Graphtec WR7500), and the water tem-

perature as measured in the supply tank was noted. Subsequently, peak-to-peak pressure amplitude and oscillation frequency were determined from the recordings.

RESULTS AND DISCUSSION

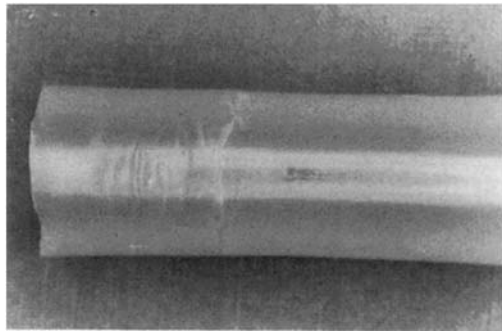
The experimental values of Young’s modulus, mean air pressure, minimum and maximum water temperature, and the angle of the oscillatory plane of the tube with respect to gravity are shown in Table II. The Young’s modulus of the tube material was measured as varying between 3.27 and 4.56 MPa, with an average value of 3.82 MPa. This range includes both experimental error and apparently genuine variation of the tube properties between segments cut from the same bale. All other things being equal, a tube made of a stiffer material would require greater external pressure to bring about collapse and thereby initiate oscillation in the presence of flow. The mean (slight fluctuations result from the tube collapse with each oscillatory cycle) air pressure in the chamber was between 169 and 207 kPa, averaging 192 kPa.

Water temperature varied periodically with time from 14.2 to 23.8°C, excluding tube I, which was tested without the cooling system. The period ranged from 148 to 245 min, depending on ambient room temperature (18–26°C).

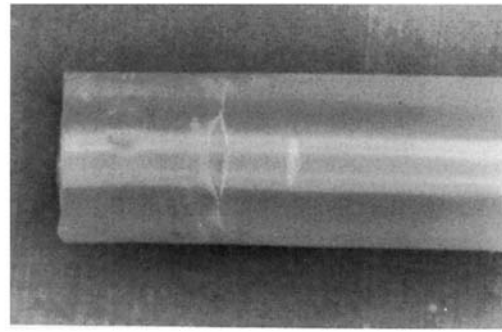
The angle of the oscillatory plane varied from tube to tube. The random oscillatory plane angle is the result of slight differences in the position of

Table III Dimensions of the Tube Scars in mm (see Fig. 4)

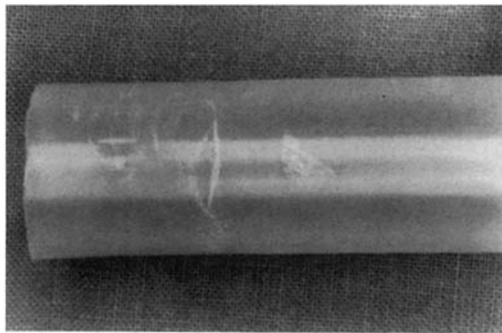
Tube	a_1	c_1	a_2	c_2	r_1	h_1	b_1	r_2	h_2	b_2
I	11.8	2.2	7	3.2	4.3	0	7.4	4.2	0	7.8
II	10.5	2.5	8.9	2.1	8.8	4.8	7.2	8.3	4.5	5.9
III	9.7	5	11.2	3.3	10	6	6.2	9.4	5.6	6.5
IV	11	2.7	10.8	2.4	9	6.1	6	8.3	5.5	7.3
V	13.3	4	9	3.7	7.3	0	6.3	7	0	7.6
VI	9.6	2.7	10	2.4	8	6.1	7	7.3	6.3	6.9
VII	12.2	4	11.4	4.3	5.7	5	6.4	6	5	7
VIII	9	4	9.8	3.5	8.5	3.9	6.3	10.3	4.3	5.8
IX	10	3	10.4	3.5	7	0	6.8	7.4	0	7
X	10.3	4.7	10	4.3	7	0	6.4	7.6	0	6.6
XI	10.6	4.3	13.8	4	6.5	6.4	6.8	7	6.5	7
XII	10.6	2.4	12.5	2.6	10	8.7	5.8	9.2	8.2	6.9
XIII	10.4	4.1	9.6	3.8	7.5	0	6.2	7.2	0	7
XIV	9.4	4	11.5	3.2	4.7	4.7	6.9	5.3	4.2	6.8
XV	12	5	12.4	3.5	5	3.6	6.7	7.5	3.6	6
XVI	14.2	3.3	12	3.8	8.3	6.3	6.5	9	6.8	5
XVII	12	2	10.5	2.8	8	5	7.2	10	6.2	5.4
XVIII	11.8	2.6	10.5	3.4	9	6.6	7	9.4	7	5.6



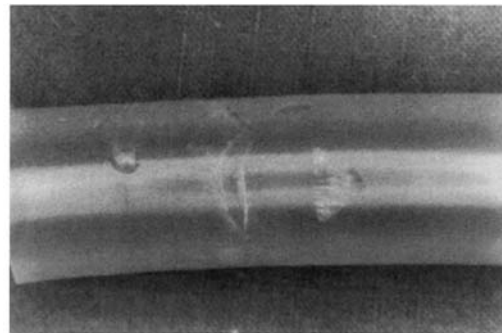
(a)



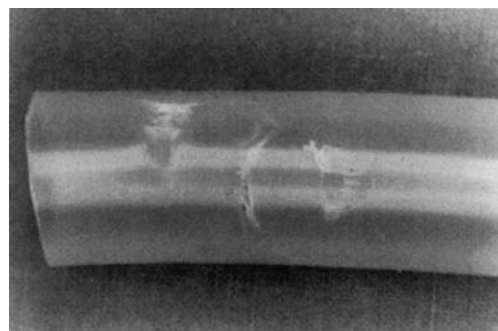
(b)



(c)



(d)



(e)

Figure 8 Photographs of the downstream end of tubes after rupture: (a) Tube X with one of two axial symmetrical surface marks formed by wall folding during collapse. The circumferential scar closest to the axial surface mark was formed at the rigid joint edge while the rest are clamp marks. (b) Tube IX with one of two symmetrical circumferential line marks formed by opposite wall contact during the tube collapse. Two circumferential lines downstream from the opposite wall contact mark are rigid joint edge scars. The tube

screw hose clamps with respect to the rigid pipes, the distance between rigid pipes (see Table I), and the tightness of clamps.

The decrease in water viscosity at higher temperature caused a decrease in the rig resistance to flow. This led to an increase in flow rate, amounting to a change in operating point for the collapsible tube oscillator, which responded by a slight increase in oscillation frequency. This in turn caused the peak-to-peak amplitude of downstream pressure variation to decrease slightly. The variations with temperature of mean flow rate, oscillation frequency, and pressure amplitude are shown in Figure 4 for all tubes with 2% longitudinal extension during their operating life. Mean flow rate increased with temperature, with an average slope of $0.5 \text{ (L/min)/}^\circ\text{C}$. Frequency increased linearly with temperature at the rate of $0.2 \text{ Hz/}^\circ\text{C}$. Peak-to-peak downstream pressure amplitude was constant for temperatures below 20°C . From 20 to 24°C , the pressure amplitude decreased with an average slope of $-11 \text{ kPa/}^\circ\text{C}$. The minimum and maximum values of mean flow rate, oscillation frequency, and pressure amplitude during all fatigue tests are presented in Figure 5.

The mean flow rate, frequency, and peak-to-peak downstream pressure amplitude did not change more than 5%, 10%, and 2%, respectively, during the whole fatigue test, excluding the first few hours. Figure 6 illustrates this behavior for tube VI.

The downstream pressure wave did not change significantly at constant temperature during the fatigue test, as shown in Figure 7 for tubes VI and XIV.

Description of the Ruptured Tubes

There were two pairs of pulsation surface marks on each tube after the fatigue test (see Fig. 3 and Table III). Longitudinal symmetrical surface marks on opposing tube wall sides at the oscillatory plane were formed by wall folding during the collapse [see Fig. 8(a)]. Each of the surface marks consisted of one

or more mainly axial lines of nonuniform thickness. Another pair of symmetrical surface marks was located at 90 degrees with respect to the wall-folding surface marks. These marks formed as the result of contact between the inside tube walls during the tube collapse. They consisted of (1) circumferential lines for tubes I, V, IX and XIII [see Fig. 8(b)]; (2) a group of fine axial or inclined lines for tubes VI, VII, VIII, X and XIV [see Fig. 8(c)]; and (3) a group of fine axial or inclined lines forming a triangular area for tubes II, III, IV, XI, XII, XV, XVI, XVII and XVIII [see Figs. 8(d) and 8(e)].

All tubes mounted on an 18.0-mm-diameter pipe downstream ruptured at the edge of the downstream joint [see Figs. 8(b), 8(c), and 8(d)]. The tubes mounted on a 14.5-mm diameter pipe downstream ruptured at the same place (XII, XV, XVI, and XVIII) or at one of the scars (XIII, XIV, and XVII), as a result of contact between the inside tube walls during tube collapse [see Fig. 8(e)]. The rupture of the tubes at the downstream rigid pipe edge occurred in spite of careful rounding and polishing of the downstream pipe entrance.

The Operating Life of the Silicone-Rubber Tube Oscillator

The operating life of the silicone-rubber tubes is presented in Figure 9. It varied from 146 h (tube XIV) to 378 h (tube VIII). The total number of oscillations was between 3.48 and 9.67 million. The reduction of the outside diameter of the downstream joint from 18.0 to 14.5 mm did not influence the tube's operating life. This was contrary to the initial expectation that a smaller diameter would lead to a longer operating life, since the reduced circumferential tube stretch gave greater tube wall thickness at the downstream joint entrance as well as reduced tearing stress. The variations in operating life of the tubes were uncorrelated with Young's modulus, or with amplitude or frequency of oscillation.

was ruptured through the scar closer to the opposite wall contact mark. (c) Tube VI with one of two symmetrical groups of fine inclined line marks as the result of opposite wall contact during the tube collapse. The two circumferential lines downstream from this marks are pipe-edge scars. The tube ruptured at the scar closer to the opposite wall contact marks. (d) Tube IV with one of two symmetrical groups of fine inclined line marks forming a triangular area as the result of opposite wall contact during the tube collapse. The two circumferential lines downstream from this marks are pipe-edge scars. The tube ruptured at the scar closer to the opposite wall contact marks. (e) Tube XVII with one of two symmetrical groups of fine inclined line marks forming a triangular area as the result of opposite wall contact during tube collapse. The thick inclined line originating from the triangle is where the tube split. The circumferential line downstream from the opposite wall contact marks is a rigid joint edge scar.

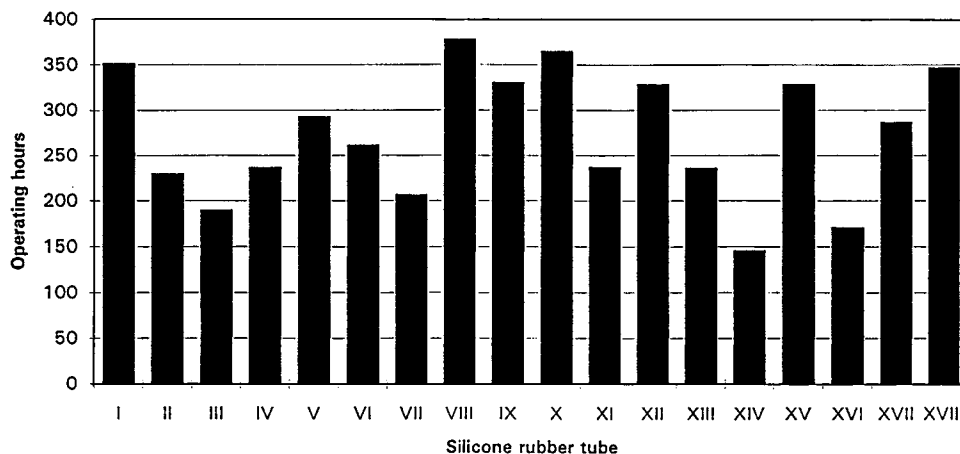


Figure 9 The operating life of the silicone-rubber tube oscillators.

Lubrication of the downstream rigid pipe edge might prolong the life of a silicone-rubber tube. However, any lubricant would contaminate the feedstock.

The effects of tube rupture in the context of an industrial plant need not be damaging to throughput. Two parallel silicone-rubber collapsible tube pulsation generators could be installed in a commercial rig. One of them would be active while the other was in reserve. Failure of the silicone-rubber tube does not cause any leakage of the feedstock suspension because the compressed air penetrates through the fine tube rupture into the liquid. The oscillations stop and partly aerated liquid passes through the tube. The failure can be indicated by a pressure transducer or flow-rate meter or by an ultrasonic bubble detector. The parallel pulsation generator with unused silicone-rubber tube can be activated while the pulsation generator with ruptured tube is isolated.

The collapsible-tube pulsation generator is inherently an extremely simple, cheap, and reliable device and has low running costs. These advantages, once demonstrated to the satisfaction of the membrane separation community, could lead to the more widespread adoption of pulsatile feed flow where membrane flux maximization is needed. Potential benefits are not confined to the field of filtration, since the principle is applicable to many different areas of heat and mass transfer where a boundary layer limits the diffusion rate.

CONCLUSIONS

Fatigue tests have shown that a silicone-rubber tube can be used as the active element of a cheap and

reliable oscillator with good reproducibility of the downstream pressure. The operating life of the 18 tubes tested was between 146 and 378 h of continuous work for peak-to-peak downstream pressure amplitude 220 to 310 kPa and frequency 5.2 to 8.5 Hz.

We thank the Australian Research Council for its financial support.

REFERENCES

1. M. F. Edwards and W. L. Wilkinson, *Trans. Instn Chem. Engrs.*, **49**, 85 (1971).
2. D. A. Colman and W. S. Mitchell, *J. Chem. E. Symp. Series*, **118**, 119 (1990).
3. K. Abel, M. A. Jaffree, B. J. Bellhouse, E. L. Bellhouse, and W. S. Howarth, *Trans. Am. Soc. Artif. Intern. Organs*, **27**, 639 (1981).
4. S. M. Finningan and J. A. Howell, *Chem. Eng. Res. Des.*, **67**, 278 (1989).
5. J. W. Stairmand, B. J. Bellhouse, Z. Jamal, R. W. H. Lewis, J. P. Urban, and C. C. Entwistle, *Life Support Systems*, **4**, 193 (1986).
6. V. Milisic and J. L. Bersillon, *Filtr. Sep.*, **23**, 347 (1986).
7. V. D. J. Rodgers and R. E. Sparks, *AICh. E. J.* **37**, 1517 (1991).
8. V. D. J. Rodgers and R. E. Sparks, *J. Membrane Sci.*, **68**, 149 (1992).
9. V. D. J. Rodgers and R. E. Sparks, *J. Membrane Sci.*, **78**, 163 (1993).
10. M. Y. Jaffrin, L. H. Ding, and B. B. Gupta, *Life Support Systems*, **5**, 267 (1987).
11. R. Ben Amar, A. K. Bouzaza, M. Y. Jaffrin, and B. B. Gupta, *Progres Dans Les Techniques de Separation et de Melange*, **1**(2), 1. Lavoisier Technique et Documentation, Paris, 1987.

12. T. J. Kennedy, R. I. Merson, and B. J. McCoy, *Chem. Eng. Sci.*, **29**, 1927 (1974).
13. S. Ilias and R. Govind, *Separation Sci. & Technol.*, **25**, 1307 (1990).
14. H. Bauser, H. Chmiel, N. Stroh, and E. Walitza, *J. Membrane Sci.*, **11**, 321 (1982).
15. B. B. Gupta, P. Blanpain, and M. Y. Jaffrin, *J. Membrane Sci.*, **70**, 257 (1992).
16. H. G. Liu and R. Ben Aim, Proc. IMSTEC '92 Conf., Sydney, November 10–12, Centre for Membrane Science and Technology, The New South Wales University, Kensington, NSW, Australia, 1992.
17. I. G. Wenten, D. M. Koenhen, H. D. W. Roesink, A. Rasmussen, and G. Jonsson, *Engineering of Membrane Process II, Environmental Applications*, April 26–28, 1994, II Ciocco, Tuscany, Italy.
18. C. D. Bertram, M. R. Hoogland, H. Li, R. A. Odell, and A. G. Fane, *J. Membrane Sci.*, **84**, 279 (1993).
19. C. D. Bertram, *J. Biomech.*, **20**, 863 (1987).
20. C. D. Bertram, C. J. Raymond, and T. J. Pedley, *J. Fluids & Structures*, **4**, 125 (1990).
21. C. D. Bertram and K. S. A. Butcher, *J. Fluids & Structures*, **6**, 163 (1992).
22. C. D. Bertram, M. D. Sheppeard, and O. E. Jensen, *J. Fluids & Structures*, **8**, 673 (1994).

Received October 6, 1995

Accepted January 24, 1996